Electronic Supplementary Material (ESI) for Chemical Communications

Supporting Information

Organic Nanowire/Metal Nanoparticle Hybrid for the Highly Enhanced Fluorescence Detection of Dopamine

Yingzhi Chen, Jun Yang, Xuemei Ou, Xiaohong Zhang*

† Nano-organic Photoelectronic Laboratory and Key Laboratory of Photochemical Conversion and Optoelectronic Materials, Technical Institute of Physics and Chemistry, Chinese Academy of Science, Beijing 100190, China

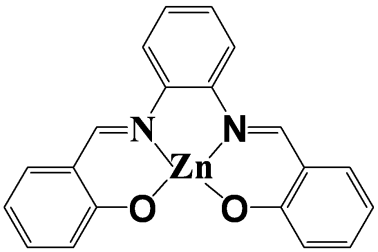

Molecular Structure of Zinc–salophen

S1, Fabrication of Zinc–salophen (ZnSa) complex nanowires (NWs), ZnSa NWs/Ag nanoparticles (NPs) hybrid nanostructures I, II and III. ZnSa complex was synthesized as described in ref.[S1] Self-assembly of ZnSa into NWs was performed through direct vaporization. A drop of THF/DMF solution of ZnSa (20 mM) was allowed to evaporate on silicon substrate at room temperature. The volume ratio of THF and DMF was 2:3. Due to the low evaporation rate of DMF, the self-assembly proceeded slowly and NWs up to several μm were therefore obtained. As shown in inset of Figure S1A, the morphology of the obtained ZnSa was wire-like in structure with diameters between 100 nm to 300 nm and lengths of up to several micrometers. In addition, the nanowires had very smooth surfaces with little impurities or crystal defects.

Assembly of the NW/NP hybrid was realized through a simple wet-chemical method. The detailed experimental process was as follows.

2 mg of the obtained NWs were dispersed in $AgNO_3$ solution (5 mM, 10 mL) and stirred for 1d to ensure the efficient absorption of Ag^+ ions on the NWs surface. Addition of $NaBH_4$ (0.5 M, 100 μL) ensued to reduce the Ag^+ ions. The reaction remained half day to allow the good seeding and aggregation, hence hybrid III with a homogeneous distribution of Ag NPs were produced. The products were purified by centrifugation in distilled water. SEM measurement was performed with a Hitachi S-4300 (operated at 10 kV). The sample was prepared by casting one drop of hybrid suspension in water onto a silicon wafer, followed by drying in air and annealing overnight in an oven at 50 ^oC , and then observed under SEM, as shown in Figure S1C. The layer of NPs on the ZnSa NWs was confirmed by energy dispersive X-ray

spectra (EDS) to be Ag particles (Figure S1D).The separation distance between Ag NPs was about 20nm, seen in inset of Figure 1C.

2mg of the obtained NWs were dispersed in $AgNO_3$ solution (3 mM, 10 mL) and (1 mM, 10 mL), respectively. Both mixtures were stirred for 1d, followed by the reduction of $NaBH_4$ (0.5 M, 100 μL) to form hybrid II, I. The products finally obtained were shown in Figure S1A, S1B, featuring a larger separation distance (about 50 nm-100 nm) than hybrid III.

Here, the electron-donating ZnSa NWs may serve not only as a surface template for attracting Ag^+ ions to selectively nucleate Ag seeds[S2] as binding sites but also a support for the growth of Ag NPs during $NaBH_4$ reduction. When the $AgNO_3$ concentration was increased, the amount of Ag seeds deposited onto the NWs tended to increase; thus, Ag NPs with higher densities might be expected along the surface of NWs after reduction, and vice versa.

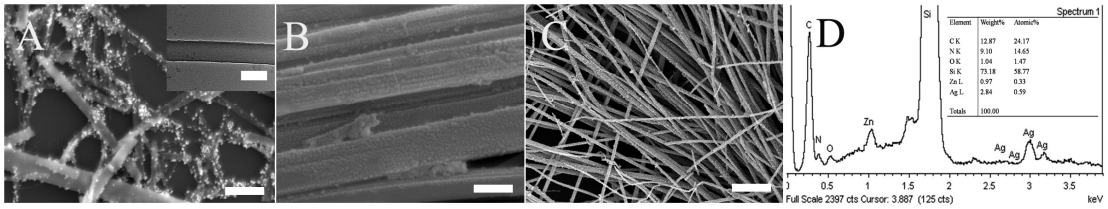

Figure S1. SEM images of hybrid I (A), II (B) and III (C) in a large scale, TEM image of ZnSa NW (inset in A) and EDS spectrum in SEM experiments for the hybrid III (D). Scale bars are 500 nm, 100 nm, 500 nm, and inset in A is 100 nm.

S2, Fluorescence measurement of ZnSa free molecules, ZnSa NWs and hybrids. The fluorescence spectra shows the emission difference between ZnSa free molecules and ZnSa NWs, as shown in Figure S2.1. Upon aggregation, the emission of individual molecules, centered at 412 nm, disappeared, while a significant, red-shifted emission at 523 nm was measured, characteristic of strong intermolecular electronic interaction typically observed in molecular aggregates.[S3] No emission of individual molecules was detected for the ZnSa NW suspension, implying that all the molecules were assembled into aggregates. The significant difference in emission peaks between ZnSa free molecules and NWs provides a good opportunity to study the aggregation-deaggregation behaviors of the hybrid and the favorable detecting results brought about by these behaviors.

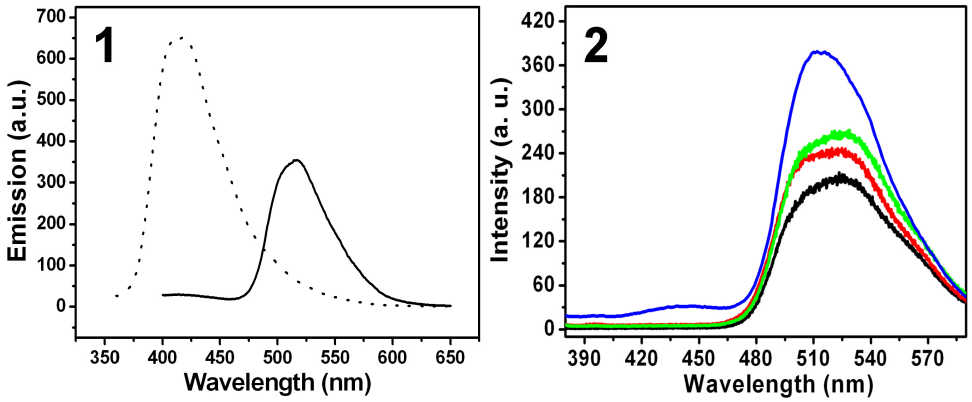

Figure S2. 1) Fluorescence spectra from ZnSa/acetone solution (about 10^{-7} M, dashed line), and from ZnSa NWs/H_2O suspension (solid line). 2) Fluorescence spectra from ZnSa NWs (black), ZnSa NWs/Ag NPs hybrid I (red), hybrid II (green), and hybrid III (blue).

S3, Determination of surface Plasmon (SP) energy of hybrid nanostructures I, II and III. To measure the SP energy of the adsorbed Ag NPs, UV-vis absorption spectra was recorded with a Hitachi UV-3010 PC spectrophotometer. Ag NPs were separated from NWs after the addition of large amount of acetone (100 mL) by centrifugation. The UV-vis absorption spectrum (Figure S3) shows their absorption peaks, representing SP energy. Absorption peaks at 382 nm, 385 nm, and 392nm were observed for Ag NPs in hybrids I, II, and III, respectively. The peaks showed a small red-shift in absorption as the size of Ag NPs increased.

The SPR-assisted fluorescence enhancement was supported by the UV-vis absorbance spectra of Ag NPs. Excitation of SPs by light at an incident wavelength (350 nm), near SP energy, where resonance occurs, results in SPR coupling between Ag NPs and vicinal ZnSa fluorophores and contributes to effective energy transfer. Through energy transfer during SPR coupling,[S4] the number of excitons for the band gap emission of ZnSa increases and fluorescence enhancement can be achieved. The plasmon resonances of NPs that are tuned to the emission wavelength of the fluorophore have been proven to show maximum fluorescence enhancement.[S5] Resonance coupling of fluorescence emission (412 nm) with surface plasmons (380~390 nm), where plasmons efficiently and quickly radiate the coupled emission, could be expected to result in an outstanding increase in the radiative decay rate of the fluorophore and enhanced emission intensity. Consequently, the emission intensity of

the hybrids at 412 nm gained a great enhancement when DA was added.

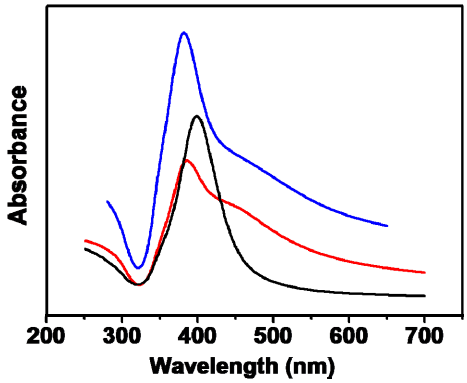

Figure S3. UV/V is absorption spectra of hybrid I (blue), II (red) and III (black).

S4, Illustration of the coordination-assisted deaggregation.

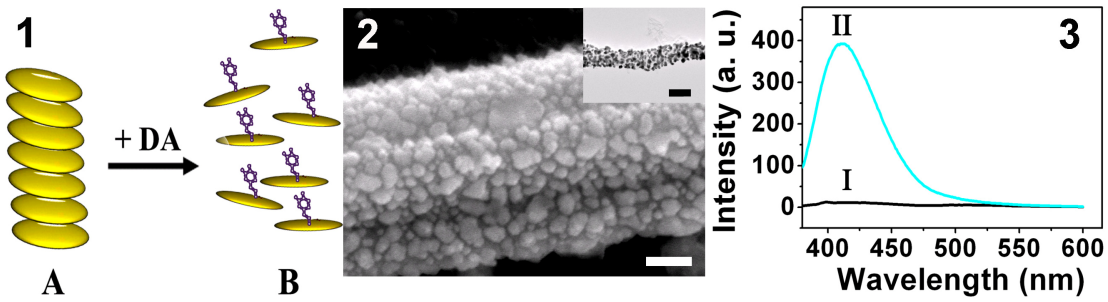

Figure S4. 1) Illustration of coordination-assisted deaggregation. A: ZnSa aggregates on surficial ZnSa NWs. B: ZnSa free molecules with DA. 2) SEM and TEM image (inset in 2) of the hybrid III after fluorescence binding to DA. Scale bar is 50 nm, and inset in 2 is 100 nm. 3) Fluorescence spectra of the solution after removal of the hybrid III from H_2O (I), and from DA solution (II).

The deaggregation behavior was illustrated in Figure S4.1. Addition of DA that could coordinate to ZnSa bond firmly to ZnSa aggregates on the surficial ZnSa NWs. Such coordinating force readily interrupted the aggregation of surficial ZnSa aggregates and ZnSa free molecules were thus released from it. From Figure S4.2, the minimal amount of DA didn't cause much damage on the overall morphology of the hybrid structure, because it only acted on the small part surficial ZnSa aggregates. As it indicated in Figure S4.3, the only one peak at 412 nm after removal of the coordinated hybrid actually proved the release of free ZnSa molecules when subject to coordination-assisted deaggregation.

S5, Sensitivity and temporal stability of hybrid III for DA detection.

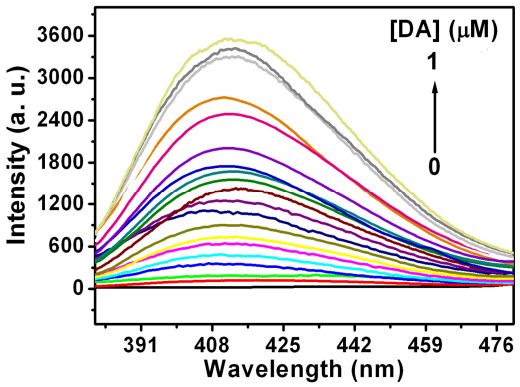

Figure S5. Fluorescence spectra of hybrid III in the presence of increasing DA concentrations (0-1 μM).

Fluorescence spectra analysis (Figure S5) showed that surficial ZnSa assembly deaggregated with the addition of DA, and this deaggregation process was thought to undergo 3 steps: pre-deaggregation, deaggregation, monodisperse. As shown in Figure 3.1, pre-deaggregation happened at the DA concentration below 400 nM, during which the addition of DA led to only a small degree of deaggregation and thus a slight increase of I_{412}, but did not disrupt the aggregated state of surficial ZnSa assembly. At the DA concentration ranging from 400 nM to 600 nM, DA readily interrupted the ZnSa aggregates. Herein, ZnSa assembly deaggregated massively with the addition of DA, and resulted in an abrupt increase of I_{412}. As more DA was added, surficial deaggregation finished and I_{412} reached a plateau.

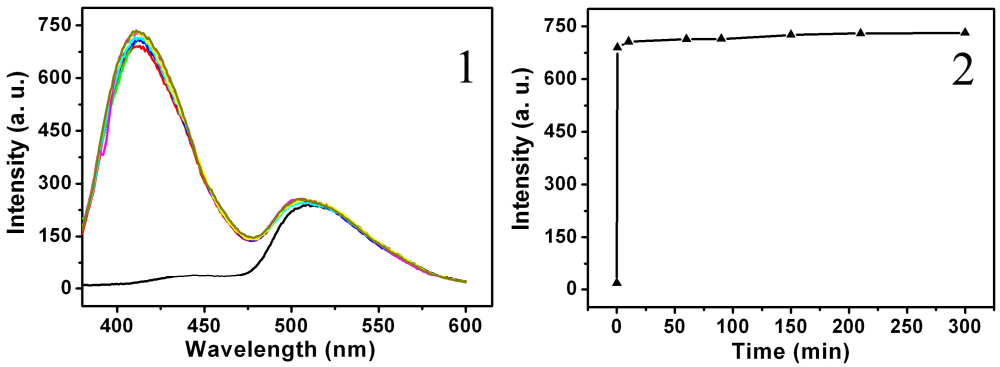

Figure S6. 1) Fluorescence intensity of hybrid III /DA solution (1 mg/0.2 μM) at 412 nm over time UV irradiation at 365 nm. 2) Plots of the fluorescence intensity hybrid III/DA solution (1 mg/0.2 μM) at 412 nm as a function of time.

S6, Fluorescent detection for dopamine (DA) from mixture of Ag NPs and ZnSa NWs. 3mg Ag NPs were mixed with 2 mg ZnSa NWs to study its response to DA.

The fluorescence measurement was performed in a cuvette (5 mL volume), into which 3 mL DA solution (1.0 mM) was added and stirred homogeneously. As shown in Figure S7, a second very weak emission at 412 nm was observed when DA was added to the mixture. The result showed that only close combination of Ag NPs and ZnSa NWs enabled greatly enhanced fluorescence detection of DA; the large distance between ZnSa NWs and Ag NPs from their simple mixing did not make it because it was supposed to generate little SPR.

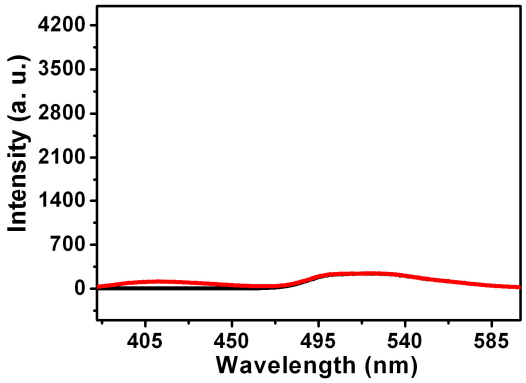

Figure S7. Fluorescence spectra of the mixture of Ag NPs and ZnSa NWs upon DA addition.

S7, Sample stability of hybrid III for different samples. Hybrid III sample was divided into five aliquots (1 mg) to measure their response stability for DA detection. When DA (0.25 μM, 3 ml) was separately added into the five aliquots, only a small detection variation was observed, as shown in Figure S8, indicating a homogenous distribution of Ag coverage and thus a good sample stability.

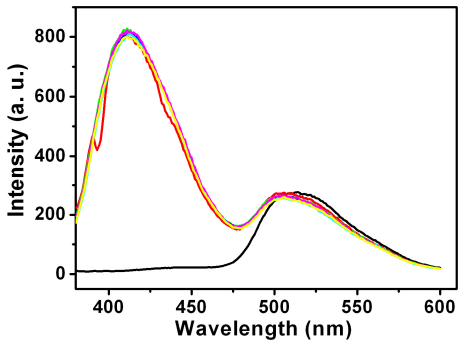

Figure S8. Fluorescence emission of five aliquots of hybrid III solution in response to DA (0.25 μM, 3 ml).

S8, Specificity for DA under the foreign interference. Hybrid III solution was presented in DA or other analytes (3 mL, 1 μM) to test whether sensor hybrid III was specific for DA detection. It is worthy to note that addition of serotonin, another neurotransmitter like DA, caused a weaker fluorescence enhancement than DA, and

this could be ascribed to the much bulkier structure of serotonin and thus weakened interaction with the aggregated nanowires. The result shows that our proposed hybrid demonstrates superior selectivity toward DA over other interferences.

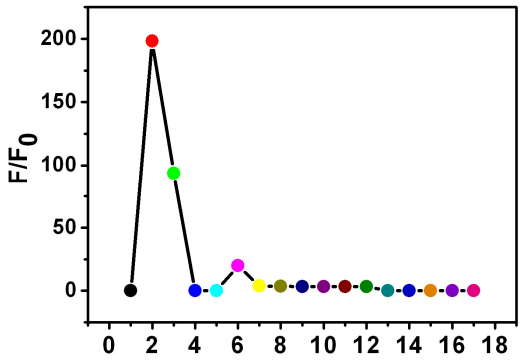

Figure S9. Fluorescence response of hybrids III in blank (1), and in the presence of 1 μM DA (2), Serotonin (3), Ascorbic acid (4), Uric acid (5), Glycine (6), Alanine (7), Valine (8), Leucine (9), Glutamic acid (10), Aspartic acid (11), Tyrosine (12), Lactose (13), Glucose (14), Na^+ (15), K^+ (16), Zn^{2+} (17). F/F_0: I_{412} of hybrids III in chosen sample solution (3ml, 1 μM) versus that in H_2O.

S9, Effect of pH on performance of sensor hybrid III. To further study the proposed sensing mechanism and the practicality of the method, the effects of pH on the fluorescent response to DA of the hybrid III were also investigated. The pH dependence was measured in a solution containing 0.1M KNO_3 and 0.01M borate buffer. The pH of this solution was adjusted with 0.1M KOH or 0.1M HNO_3. Experimental results show that upon addition of DA, hybrid III shows different F/F_0 enhancements. Under acidic conditions (pH<6), the DA maybe partially protonated, which decreases the coordinating interaction between DA and ZnSa. At pH over 9, the DA maybe partially oxidized, which can also weaken the coordinating interaction between DA and ZnSa. Sensor hybrid III shows the highest fluorescence response toward DA in the pH range of 6.0-8.0. Neutral pH was thought as the optimum experimental condition.

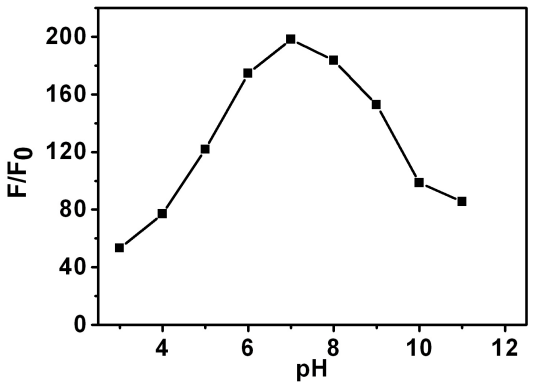

Figure S10. Effect of pH on the fluorescence response (F/F_0) of hybrid III in response to DA (3ml, 1 μM) at room temperature. F/F_0: I_{412} of hybrids III with DA (3ml, 1 μM) versus that without DA at one specified pH.

References

S1 A. Singer, D. Atwood, *Inorg.Chim.Acta*, 1998, **277**, 157.

S2 H. Chu, J. Wang, L. Ding, D. Yuan, Y. Zhang, J. Liu, Y. Li, *J. Am. Chem. Soc.*, 2009, **131**, 14310.

S3 C. T. L. Ma, M. J. MacLachlan, *Angew. Chem. Int. Ed.*, 2005, **44**, 4178.

S4 J. Joo, D. H. Park, M. Y. Jeong, Y. B. Lee, H. S. Kim, W. J. Choi, Q. H. Park, H. J. Kim, D. C. Kim, J. Kim, *Adv. Mater.*, 2007, **19**, 2824.

S5 a)F. Tam, G. P. Goodrich, B. R. Johnson, N. J. Halas, *Nano Lett.*, 2007, **7**, 496; b)R. Bardhan, N. K. Grady, J. R. Cole, A. Joshi, N. J. Halas, *ACS Nano*, 2009, **3**, 744.